

# Kinetic study of electrochemical reactions at catalyst-recast ionomer interfaces from thin active layer modelling

F. GLOAGUEN, F. ANDOLFATTO, R. DURAND, P. OZIL

CREMGP/ENSEEG, BP 75, 38402 Saint Martin d'Hères, France

Received 5 November 1993; revised 21 February 1994

The objective of the following study was to test proton exchange membrane fuel cell catalysts. A mixture of supported catalyst and recast ionomer (Nafion<sup>®</sup>) was deposited on a rotating disc electrode (RDE). The resulting thin active layer was immersed in a dilute sulphuric acid solution. The RDE technique allows correction of mass transfer limitation in solution. To calculate the kinetic parameters from the current–potential relation, a mathematical model was written taking into account gas diffusion, ohmic drops and interfacial kinetics within the thin layer. Analytic and/or numerical expressions for the effectiveness factor and for the current–potential relation were obtained. The oxygen reduction reaction at various Pt/C-recast Nafion<sup>®</sup> interfaces demonstrates the validity of this test procedure.

## Nomenclature

$b$	Tafel slope ( $\text{V dec}^{-1}$ )
$c$	Local gas concentration ( $\text{mol cm}^{-3}$ )
$c_s$	gas concentration at the electrolyte side ( $\text{mol cm}^{-3}$ )
$\bar{D}$	gas diffusion coefficient within the layer ( $\text{cm}^2 \text{s}^{-1}$ )
$F$	Faraday constant ( $96\,500 \text{ C mol}^{-1}$ )
$i$	total current density based on the geometric area ( $\text{A cm}^{-2}$ )
$i_0^*$	exchange current density per real catalyst area ( $\text{A cm}^{-2}$ )
$I$	dimensionless total current density
$j$	local ionic current density based on the geometric area ( $\text{A cm}^{-2}$ )
$\bar{K}$	ionic conductivity within the layer ( $\text{S cm}^{-1}$ )
$\bar{K}_e$	electronic conductivity within the layer ( $\text{S cm}^{-1}$ )

$L$	layer thickness (cm)
$m$	mass fraction of catalyst in the catalytic powder
$n$	total number of electrons involved in reaction
$R$	gas constant ( $8.31 \text{ J K}^{-1} \text{ mol}^{-1}$ )
$S$	specific catalyst area ( $\text{m}^2 \text{ g}^{-1}$ )
$T$	temperature (K)
$u, v$ and $w$	dimensionless parameters in Equations 8 and A4
$y$	dimensionless abscissa

## Greek symbols

$\alpha$	cathodic transfer coefficient
$\epsilon$	effectiveness factor
$\phi$	local dimensionless overpotential
$\gamma$	real catalyst area/geometric area ratio
$\eta$	local overpotential (V)
$\theta$	Nafion <sup>®</sup> volume fraction
$\tau$	tortuosity factor

## 1. Introduction

Measurements of reaction kinetics are important for evaluating proton exchange membrane fuel cell behaviour and for adjusting the experimental parameters to improve the catalyst utilisation. Due to the complex structure of a porous gas electrode (usually composed of a porous backing and an active layer), it is not easy to separate the kinetic limitation from the overall limitation. In the field of gas-phase heterogeneous catalysis, Thiele [1] and Wheeler [2], however, showed that the mass transport of reactant within catalytic porous pellets of controlled and reproducible geometry, could be accounted for to provide analytical expressions for the apparent

reaction rate. Using an analogous method, Stonehart and Ross [3] obtained the kinetic parameters of oxygen reduction and hydrogen oxidation on carbon supported platinum in phosphoric acid media using PTFE-backed thin layer flooded electrodes.

In this paper a method convenient for the study of electrochemical reaction rates at various catalyst-recast ionomer interfaces is presented. A mixture of supported catalyst (the catalytic powder) and recast Nafion<sup>®</sup> was deposited on a rotating disc electrode (RDE). The resulting thin active layer of controlled and reproducible geometry was immersed in a dilute sulphuric acid solution. The RDE technique allows correction of mass transfer limitation in solution. By analogy with the Thiele analysis, the effectiveness

factor,  $\epsilon$ , of this thin layer is calculated taking into account the ohmic and the diffusion limitations. For a given catalyst, the kinetic parameters are finally obtained by fitting the calculated current-potential relation to the experimental one. The oxygen reduction reaction (ORR) on Pt/C confirms the validity of the model.

## 2. Thin layer modelling

### 2.1. Basic equations

For kinetic parameters measurements, a compact thin layer (i.e. no void, only ionic and electronic conductors) was used. The assumption of an electrode totally flooded will have to be further confirmed during the experiment. In the mathematical modelling of flooded electrodes, the macroscopic analysis [4–6] allows simplification of some assumptions, while maintaining practical and physical significance. Here, the thin active layer is treated as a superposition of two continua, one representing the recast Nafion<sup>®</sup> phase (the ionic conductor) and the other the catalytic powder (the electronic conductor). Both are present at any point in the space.

When the catalytic powder consists of small carbon supported platinum particles, it is convenient to characterize the porous electrode geometry by  $\gamma$ , the total catalyst area/geometric area ratio. This ratio is directly obtained from electrochemical measurements (see Section 3). For a flooded electrode of slab geometry and thickness  $L$  as sketched in Fig. 1, the various structural parameters are linked by the relation:

$$\frac{\gamma}{L} = (1 - \theta)\rho m S \times 10^4 \quad (1)$$

where  $S(\text{m}^2 \text{g}^{-1})$  is the specific area of the catalyst,  $\theta$  the volume fraction of Nafion<sup>®</sup>,  $\rho$  ( $\text{g cm}^{-3}$ ) the catalytic powder density and  $m$  the mass fraction of the supported catalyst.

One side of the active layer is in contact with a current collector ( $x = L$ ) and the other ( $x = 0$ ) with a sulphuric acid solution containing the dissolved reactant. The reactant diffuses into the Nafion<sup>®</sup> phase and reacts simultaneously at the catalyst interfaces. It was assumed that the isothermal and steady state conditions apply and that the governing equations are reduced to a one-dimensional form.

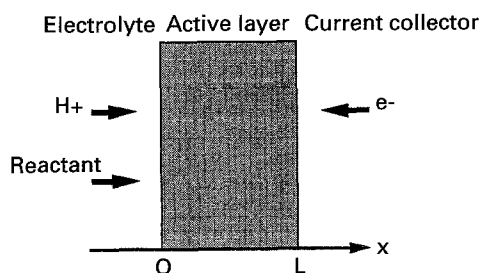


Fig. 1. Totally flooded cathode model used in the theoretical analysis of the thin active layer.

At the cathode for example, by assuming Tafel kinetics,  $i^*(x)$ , the rate of the electrochemical reaction per real catalyst area unit is related to the derivative of  $j(x)$ , the ionic current density per geometric area unit as

$$\frac{dj}{dx} = \frac{\gamma}{L} i^*(x) = -\frac{\gamma}{L} i_0^* \left\{ \frac{c(x)}{c(0)} \exp \left[ \frac{-\alpha F \eta(x)}{RT} \right] \right\} \quad (2)$$

where  $i^*(x) < 0$ ;  $i_0^*$  is the exchange current density per real catalyst area,  $c(x)$  the local concentration,  $c(0) = c_s$  the solubility of the reactant in Nafion<sup>®</sup>,  $\eta(x) (< 0)$  the overpotential and  $\alpha$  is the cathodic transfer coefficient. From Fig. 1,  $j(x)$  is positive and  $dj/dx$  negative. The boundary conditions required for solving the above differential equation are

$$j(0) = i; \quad \eta(0) = \eta_s; \quad c(0) = c_s \quad \text{at } x = 0 \quad (3)$$

$$j(L) = 0 \quad \text{at } x = L \quad (4)$$

where  $i$  is the total current density generated by the electrode for a given overpotential  $\eta_s$ . Using Ohm's law for the ionic conduction and assuming a very large electronic conductivity, the following relation is obtained:

$$\frac{d\eta}{dx} = \frac{j(x)}{K} \quad (5)$$

More general treatment, taking into account electronic conductivity, is given in the appendix. By using Fick's law, the reactant balance over a differential element  $dx$  leads to

$$\frac{dc}{dx} = -\frac{j(x)}{nFD} \quad (6)$$

In the active layer, the effective gas diffusion coefficient,  $\bar{D}$ , and the effective proton conductivity,  $\bar{K}$ , are constant and both smaller than in bulk Nafion<sup>®</sup>, because the volume fraction of the conducting medium ( $\theta$  for the Nafion<sup>®</sup> phase) must be taken into account. If  $x$  is the linear dimension, the actual path length is  $\tau x$  where  $\tau$  is a tortuosity factor. Hence,

$$\bar{D} = \frac{\theta}{\tau} D_{(\text{bulk Nafion}^{\text{®}})}; \quad \bar{K} = \frac{\theta}{\tau} K_{(\text{bulk Nafion}^{\text{®}})} \quad (7)$$

Equations 2, 5 and 6 may be transformed into analogous dimensionless ones by using the following substitutions:

$$y = x/L; \quad \phi = -\alpha F \eta / RT; \quad C = c/c_s$$

Separating the variables leads to the following differential equation:

$$\frac{d^2 C}{dy^2} = u C \exp \left[ \frac{v}{u} (C - 1) + \phi(0) \right] \quad (8)$$

where

$$u = \frac{i_0^* \gamma L}{nFD C_s} \quad \text{and} \quad \frac{i_0^* \gamma L \alpha F}{KRT} \quad (9)$$

From Equations 3 to 6, the boundary conditions of Equation 8 may be rewritten as

$$\left(\frac{dC}{dy}\right)_0 = -uI; \quad \phi(0) = \phi_s; \quad C(0) = 1 \quad \text{at } y = 0 \quad (3a)$$

$$\left(\frac{dC}{dy}\right)_1 = 0 \quad \text{at } y = 1 \quad (4a)$$

where  $I = i/i_0^* \gamma$  is the total dimensionless current and  $\phi_s = -\alpha F \eta_s / RT$  the corresponding dimensionless overpotential.

## 2.2. Analytical and numerical solutions

At this point, the utilization of the catalyst is most interesting, not the concentration distribution or the current overpotential relation. The effectiveness factor,  $\epsilon$ , was then calculated using the following definition:

$$\epsilon = \frac{\text{actual rate (current density)}}{\text{rate (current density) without mass and ohmic limitations}} \quad (10)$$

$\epsilon$  is a function of kinetic parameters  $i_0^*$ ,  $\alpha$ , geometric parameters  $L$ ,  $\theta$ ,  $\tau$ ,  $\gamma$  and transport parameters  $Dc_s$ ,  $K$ . When the ohmic and diffusion limitations are negligible,  $\epsilon$  is close to unity and the catalyst in the porous electrode works uniformly.

**2.2.1. Analytical solution.** In Equation 8, the higher absolute value of  $v \times (C - 1)/u$  is

$$\frac{v}{u} = \frac{\alpha n F^2 Dc_s}{RTK} \quad (11)$$

For recast Nafion<sup>®</sup>,  $K \approx 0.05 \text{ S cm}^{-1}$  [7] and  $(\alpha n F^2)/(RTK)$  is then of the order of  $10^8 \text{ cm s mol}^{-1}$ . For low values of the product  $Dc_s$  (which is typically the case for hydrogen and oxygen:  $Dc_s$  is of the order of  $10^{-11} \text{ mol cm}^{-1} \text{ s}^{-1}$  [8–11]),  $v/u$  is much lower than  $\phi_s$  for a practical range of overpotentials. Then Equation 8 is reduced to

$$\frac{d^2 C}{dy^2} = \{u \exp(\phi_s)\} C \quad (12)$$

Solving Equation 12 with the boundary conditions (3a) and (4a) leads to [3]:

$$\epsilon = \frac{\text{th}[\sqrt{u \exp(\phi_s)}]}{\sqrt{u \exp(\phi_s)}} \quad (13)$$

**2.2.2. Numerical solution.** For higher values of the product  $Dc_s$  (if the reactant is very soluble) and/or for lower values of ionic conductivity, the ratio  $v/u$  is no longer negligible and Equation 8 requires numerical computations for solving. Here, its solution was obtained by using the Runge–Kutta method. Since the gas concentration at the current collector site was not known, some iterations were required to determine the  $C$  value at  $y = 1$  for which

$C(0) = 1$ . When the concentration distribution within the active layer was obtained for a given overpotential, the total current density and the effectiveness factor were then calculated.

## 2.3. Strategy of fitting

Figure 2 shows that for a low reaction rate ( $i_0^* < 10^{-8} \text{ A cm}^{-2}$ ), a very thin layer ( $L \approx 1 \mu\text{m}$ ) with a high volume fraction of Nafion<sup>®</sup> ( $\theta = 0.6$ ) has an effectiveness factor greater than 0.95. Thus a Tafel plot ( $E = f(\log i)$ ) gives the kinetic parameters directly from the experimental data [12]. The transfer coefficient,  $\alpha$ , is calculated from the slope  $b (= -2.3 RT/\alpha F)$  and the real exchange current density,  $i_0^*$ , from the apparent exchange current density  $i_0 (= \gamma i_0^*)$  at the reversible potential.

When  $\epsilon \ll 1$  for practical layer thickness and/or volume fraction of Nafion<sup>®</sup>, the experimental Tafel slope increases [4] leading to an overestimate of the value of  $i_0^*$ . The correct value of the kinetic parameters, however, can still be obtained from the thin active layer modelling. The calculation of the  $i = f(E)$  relation involves the knowledge of the numerical values of the geometric transport and kinetic parameters. The geometric parameters  $\theta$ ,  $L$ ,  $\gamma$ ,  $\tau$  are experimental data and the transport parameters  $Dc_s$  and  $K$  can be determined separately (Section 3). The calculation of the kinetic parameters  $i_0^*$  and  $\alpha$  was then made by fitting the theoretical  $i = f(E)$  relation to the experimental one using the simplex method [13]. Obviously the accuracy of the calculated kinetic parameters depends on how well the physical properties of the layer are known.

## 3. Experimental details

### 3.1. Reagents

To compare theoretical calculations and experimental values, only one example of the catalyst test is presented: Platinum on Vulcan XC-72 (Cabot) from E-TEK, Inc. These powders offer a well defined average catalytic particle size and are often used in PEMFC technology. The Nafion<sup>®</sup> solution is a 5 w/w 1100 EW solution from du Pont. The 0.5 M H<sub>2</sub>SO<sub>4</sub> solutions were prepared from Suprapur Merck concentrated sulphuric acid and very pure water (Millipore super Q system). In order to decrease the sulphate anions entrance from the solution to the recast Nafion<sup>®</sup> (Donnan exclusion), some experiments were also performed in 0.1 M H<sub>2</sub>SO<sub>4</sub> solutions but the results were not very different from those obtained with the previous solutions.

### 3.2. Electrode and electrochemical instrumentation

Glassy carbon (CG) disc working electrodes (0.5 cm diam.) from Carbone Lorraine held in Kel-F<sup>®</sup>

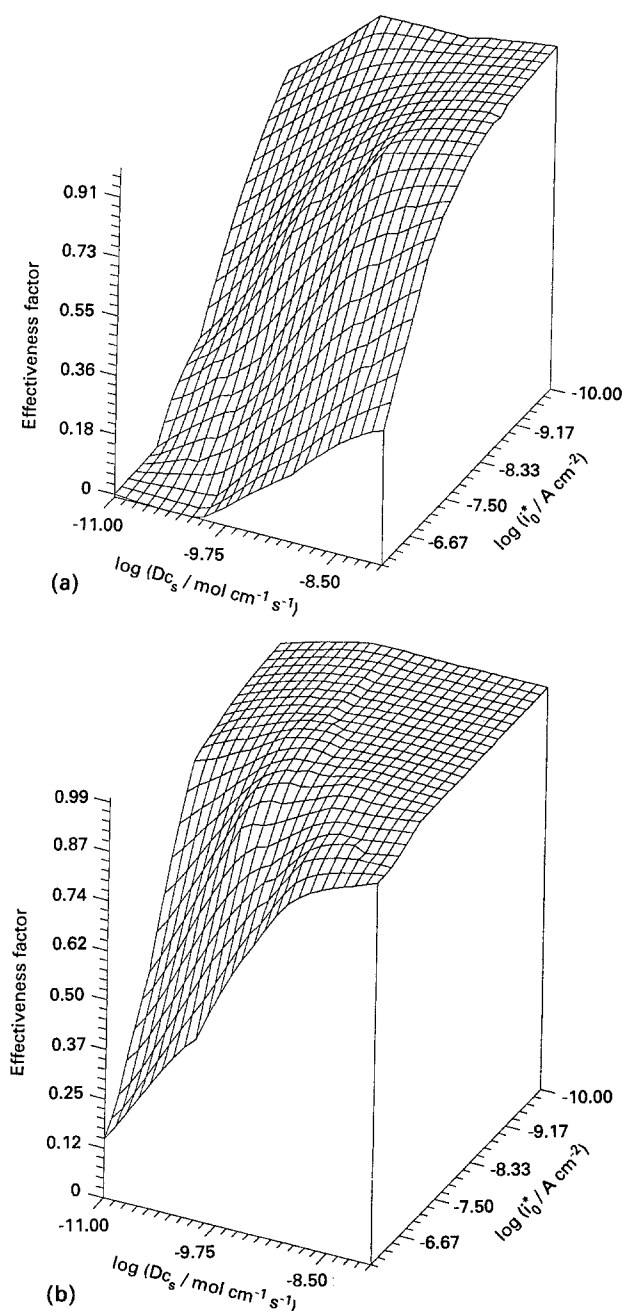


Fig. 2. Effectiveness factor as a function of  $i_0^*$  and  $Dc_s$  for various overpotentials  $\eta_s$  (a)  $= -0.4$  V; (b)  $= -0.3$  V.  $\gamma = 10$ ;  $S = 140 \text{ m}^2 \text{ g}^{-1}$ ;  $\rho = 2 \text{ g cm}^{-3}$ ;  $m = 10 \text{ wt \% Pt/C}$ ;  $\theta = 0.6$ ;  $L \approx 1 \mu\text{m}$  (according to Equation 1) and  $K = 0.05 \text{ S cm}^{-1}$ .

rods (1.1 cm diam. and 2 cm long) were used in this study. For all experiments, the working electrode was polished with  $1 \mu\text{m}$  diamond paste and then, ultrasonically cleaned in acetone, ethanol (RP Normapur Prolabo) and very pure water for 15 min prior to coating.

Electrochemical equipment included an EG & G PAR 273 potentiostat coupled via a National Instrument NI-488 interface to an HP Vectra computer. A Pyrex glass cell convenient for RDE (Tacussel EDI) technique was used. A SCE reference was connected to the cell via a Luggin capillary. Unless otherwise noted, the potentials are reported against the reversible potential taken by the Pt/C when the Nafion<sup>®</sup> phase was saturated with hydrogen.

### 3.3. Active layer coating procedures

A mixture of Pt/C, Nafion<sup>®</sup> solution, Triethylphosphate (TEP) from Merck and water was ultrasonically homogenised. Using TEP (three times the dry Nafion<sup>®</sup> mass) it was possible to heat above the glass transition temperature of Nafion<sup>®</sup> ( $140^\circ\text{C}$ ), which was necessary to obtain a well recast ionomer [14]. A measured volume of this mixture was dropped on the GC surface which allowed calculation of the final active layer thickness and its platinum loading. Low boiling point solvents were evaporated at room temperature and the whole was then heated at  $160^\circ\text{C}$  to remove TEP (Kel-F allows this heating procedure [11]). The resulting thin active layer RDE was then rinsed in water and equilibrated in  $0.5 \text{ M H}_2\text{SO}_4$  solution for 12 h prior to use.

### 3.4. Electrochemical methods

ORR for a bulk platinum RDE filmed with recast Nafion<sup>®</sup> allowed evaluation of the numerical value of the product  $Dc_s$  for bulk recast Nafion<sup>®</sup>:  $7 \times 10^{-12} \text{ mol cm}^{-1} \text{ s}^{-1}$  (this experiment is not described here, see also [10, 11]).

Cyclic voltammograms ( $0.05$  to  $1.3 \text{ V}$ ;  $0.1 \text{ V s}^{-1}$ ) recorded in a nitrogen saturated  $0.5 \text{ M H}_2\text{SO}_4$  solution were used to determine the electrochemically active platinum surface area of the thin layer by hydrogen adsorption-desorption coulometry between  $0.05$  and  $0.4 \text{ V}$  vs RHE ( $1 \text{ cm}^2$  of platinum gives  $210 \mu\text{C}$ ) [15].

The oxygen reduction current-potential curves were obtained from slow scan voltammograms ( $1.2$  to  $0.3 \text{ V}$ ;  $0.005 \text{ V s}^{-1}$ ) at various rotation frequencies ( $1000$  to  $4000 \text{ rpm}$ ) in an oxygen saturated  $0.5 \text{ M H}_2\text{SO}_4$  solution. At any potential, the cathodic current densities were corrected from mass transport in solution by calculating, for every rotation frequency  $\omega$ :  $i = i_\omega i_{L,\omega} / (i_{L,\omega} - i_\omega)$ ,  $i_\omega$  being the measured current density and  $i_{L,\omega}$  the corresponding limiting current density [12]. The resulting current-potential relations were analysed using the model and/or a direct Tafel plot.

## 4. Results and discussion

### 4.1. Voltammetry of thin active layers

The first voltammograms of freshly prepared thin active layers are sometimes featureless. With continued cycling the characteristic platinum waves rapidly develop. Successive cycles apparently clean the platinum particle surfaces within the layer and after 10 scans reproducible voltammograms were obtained (Fig. 3).

The measurement of platinum surface area in contact with Nafion<sup>®</sup> and then available to electrochemical reaction, allows the total platinum area/geometric area ratio  $\gamma$  to be obtained. Since the platinum loading of the layers was known, it was possible to estimate the specific catalyst

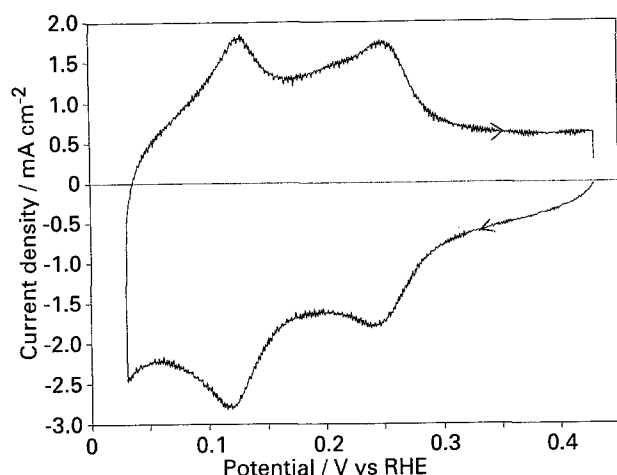


Fig. 3. Cyclic voltammograms ( $0.1 \text{ V s}^{-1}$ ) recorded after 10 scans in a nitrogen saturated  $0.5 \text{ M H}_2\text{SO}_4$  solution for a layer of Pt/C in recast Nafion<sup>®</sup>. The Pt/C from E-TEK, Inc. was a 30 wt% Pt/Vulcan XC-72 powder.  $L$ , the layer thickness, was about  $1.1 \mu\text{m}$ ;  $\gamma$ , the total catalyst area/geometric area ratio, was 27; the platinum loading  $3.4 \times 10^{-5} \text{ g cm}^{-2}$  and  $\theta$ , the volume fraction of Nafion<sup>®</sup>, was 0.6.

area  $S$  ( $\text{m}^2 \text{ g}^{-1}$ ) and the average particle size  $d$  (nm). If assuming spherical particles:  $d = 6 \times 10^3 / (21.4 \times S)$  where 21.4 is the platinum density ( $\text{g cm}^{-3}$ ). The results shown in Table 2 are in good agreement with the values given by E-TEK, Inc. [16] and estimated from direct TEM observations.

#### 4.2. Oxygen reduction reaction

Typical voltammograms for oxygen reduction on thin active layer RDE are shown in Fig. 4 and a Tafel curve directly obtained from these experimental data (i.e. only the mass transport limitation in the sulphuric acid solution is corrected) is plotted in Fig. 5. In a potential range interesting for fuel cell applications (i.e. above  $0.8 \text{ V}$ ), the Tafel slope appears, as for other acids [17], to be close to  $2.3 RT/F$ . At lower potentials, a higher slope of the order of  $2 \times 2.3 RT/F$  occurs but will not be further considered.

To confirm the theoretical calculations, ORR was investigated at two active layers of different thicknesses ( $L \approx 1.1 \mu\text{m}$  and  $L \approx 5.6 \mu\text{m}$ ). For both these thicknesses, the kinetic parameters were calculated (Table 1) using direct Tafel analysis (i.e. only the mass transport limitation in the sulphuric acid solution is corrected) and according to the model (i.e. both the mass transport limitations in the

Table 1. Kinetic parameters of ORR for a 30 wt% Pt/Vulcan in Nafion<sup>®</sup> layer

$10^4 L/\text{cm}$	$\gamma$	$10^{11} i_0^*/\text{A cm}^{-2}$	$10^3 b/V \text{ dec}^{-1}$
1.1	27	$8.4^\dagger 7.0^\ddagger$	$70^\dagger 68^\ddagger$
5.6	141	$46.0^\dagger 7.3^\ddagger$	$82^\dagger 68^\ddagger$

Above  $0.8 \text{ V}$  at  $20^\circ\text{C}$  and 1 atm.

<sup>†</sup> Directly obtained from the Tafel plot.

<sup>‡</sup> Calculated from the model with  $D_{\text{O}_2} = 7 \times 10^{-12} \text{ mol cm}^{-1} \text{ s}^{-1}$  (see Section 3).

Table 2. ORR for various Pt/Vulcan powders from E-TEK, Inc. Mass activity MA and specific activity SA as a function of the platinum particle size  $d$ . (Average values of MA and SA calculated at  $0.85 \text{ V}$ ,  $20^\circ\text{C}$  and 1 atm)

wt% Pt/C	$d/\text{nm}^\dagger$	$d/\text{nm}^\ddagger$	$SA/\mu\text{A cm}^{-2}$	$MA/\text{A g}^{-1}$
10	2.0	$2.0 (\pm 0.3)$	8.8	12.3
20	2.5	$3.2 (\pm 0.1)$	19.3	16.9
30	3.2	$3.9 (\pm 0.2)$	20.7	14.9
60	8.8	$6.0 (\pm 0.1)$	22.8	10.6

<sup>†</sup> From ref. [16].

<sup>‡</sup> Average particle size calculated from the electrochemical measurements and verified by TEM observations.

solution and within the layer are corrected). As expected, for the thinner layer ( $L \approx 1.1 \mu\text{m}$ ), the diffusion limitation within the layer is negligible and the kinetic parameters directly obtained from the Tafel plot were very close to those derived from modelling. For the thicker layer ( $L \approx 5.6 \mu\text{m}$ ) because of the diffusion limitation within the layer, the experimental Tafel slope is higher ( $|b| > 2.3 RT/\alpha F$ ) and the value of  $i_0^*$  was overestimated. After fitting, according to the model, the corrected value of  $\alpha$  and  $i_0^*$  are very close to those obtained with the thinner layer (Table 1). The validity of a totally flooded electrode model is therefore demonstrated.

At  $20^\circ\text{C}$ , 1 atm, and above  $0.8 \text{ V}$ , the exchange current density for ORR at Pt/C (30 wt% Pt/Vulcan XC-72 from E-TEK, Inc.)-recast Nafion<sup>®</sup> interface is about  $7 \times 10^{-11} \text{ A cm}^{-2}$ . The corresponding value for bulk platinum in  $1.1 \text{ N TMSA}$  is  $6 \times 10^{-11} \text{ A cm}^{-2}$  [18] and for bulk platinum in Nafion<sup>®</sup> membrane is  $2 \times 10^{-10} \text{ A cm}^{-2}$  [8].

We have also studied ORR at other Pt/Vulcan powders from E-TEK, Inc. The results are listed in Table 2 which reports mass activity, MA, and specific activity, SA, as a function of the platinum particle size. MA and SA are calculated at  $0.85 \text{ V}$ ,  $20^\circ\text{C}$  and 1 atm using

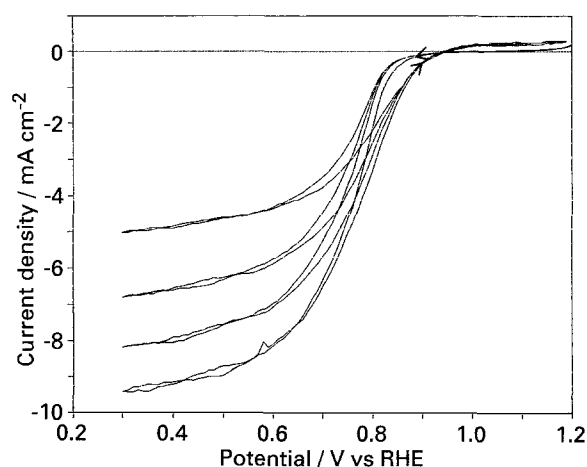


Fig. 4. Voltammograms ( $5 \text{ mV s}^{-1}$ ) recorded in an oxygen saturated  $0.5 \text{ M H}_2\text{SO}_4$  solution for a layer of Pt/C in recast Nafion<sup>®</sup>. The rotation frequencies were: (a) = 1000; (b) = 2000; (c) = 3000; (d) = 4000 rpm. Same electrode as in Fig. 3.

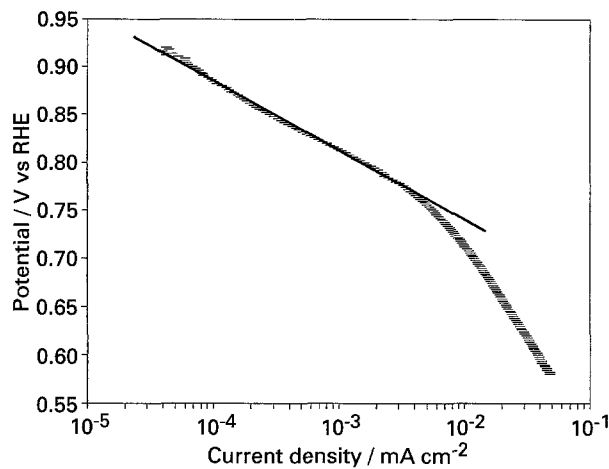


Fig. 5. Direct Tafel plot (i.e. only the mass transport in the sulphuric acid solution was corrected) for ORR at Pt/C-recast Nafion® interface. Same electrode as in Fig. 3.

$$MA = \frac{\text{current density}}{\text{Pt loading}} \text{A (g of Pt)}^{-1} \quad (15a)$$

$$SA = \frac{\text{current density}}{\gamma} \mu\text{A (cm}^2 \text{ of Pt)}^{-1} \quad (15b)$$

SA tends to increase with an increase of the platinum particle size and MA shows a maximum at a platinum particle size of about  $3.5 \pm 0.5$  nm. Fig. 2. Effectiveness Factor as a function of  $i_0^*$  and  $Dc_s$  for various overpotentials  $\eta_s$  (a) =  $-0.4$  V; (b) =  $-0.3$  V.  $\gamma = 10$ ;  $S = 140 \text{ m}^2 \text{ g}^{-1}$ ;  $\rho = 2 \text{ g cm}^{-3}$ ;  $m = 10 \text{ wt } \% \text{ Pt/C}$ ;  $\theta = 0.6$ ;  $L \approx 1 \mu\text{m}$  (according to Equation 1) and  $K = 0.05 \text{ S cm}^{-1}$ . Similar results in acid solutions led to contradictory interpretations. Kinoshita tried to correlate the rate of the oxygen reduction reaction and structural properties of the platinum particles [19]. Stonehart found no platinum particle size effect for ORR and has introduced the effect of the interparticle distance [20]. The aim of this work was to define and validate a test procedure. The results were accurate but not numerous enough to conclude on the size or the distance effects. The values of the kinetic parameters obtained from this test procedure are, however, the ones which must be considered in fuel cell applications, even if they probably include a factor due to the local geometry (nanometer scale). Other experiments with the aim of studying the effects of this geometry are presently being performed.

## 5. Conclusion

The theoretical calculations have shown that for a low reaction rate ( $i_0^*$  small) and if the active layer is thin, the kinetic parameters are directly obtained from a Tafel plot. Even for higher values of  $i_0^*$ , the model of a totally flooded electrode allows estimation of the diffusion and ohmic limitations and of the kinetic constants.

The oxygen reduction reaction on Pt/C powders demonstrates that modelling of the thin active layer as a totally flooded electrode is correct and confirms

the validity of this test procedure. The results for oxygen reduction reaction kinetics are in good agreement with previous work on bulk platinum in acid media.

## Acknowledgements

This work was supported by the ECC Joule Program. One of the authors (FG), gratefully acknowledges the ADEME for its financial support.

## References

- [1] E. Thiele, *Ind. Eng. Chem.* **31** (1939) 916.
- [2] A. Wheeler, *Adv. Catal.* **3** (1951) 249.
- [3] P. Stonehart and P. Ross, *Electrochim. Acta* **21** (1975) 441.
- [4] L. G. Austin, 'Handbook of Fuel Cell technology' (edited by C. Berger), Prentice Hall, Englewood Cliffs, N.J. (1968) p. 1.
- [5] K. Scott, *J. Appl. Electrochem.* **13** (1983) 709.
- [6] J. S. Newman, 'Electrochemical Systems', 2nd ed., Prentice Hall, Englewood Cliffs, NJ (1991) p. 454.
- [7] S. Gottesfeld, *J. Electrochem. Soc.* **139** (1992) 2980.
- [8] A. Parthasarathy, C. R. Martin and S. Srinivasan, *ibid.* **138** (1991) 916.
- [9] A. Parthasarathy, C. R. Martin, S. Srinivasan and A. J. Appleby, *ibid.* **139** (1992) 2858; *J. Electroanal. Chem.* **339** (1992) 101.
- [10] S. Gottesfeld, I.D. Raistrick and S. Srinivasan, *J. Electrochem. Soc.* **134** (1987) 1455.
- [11] D. R. Lawson, L. D. Whiteley, C. R. Martin, M. N. Szentirmay and J. I. Song, *ibid.* **135** (1988) 2247.
- [12] A. J. Bard and L. R. Faulkner, 'Electrochemical Methods', J. Wiley & Sons, New York (1980).
- [13] S. N. Deming and S. L. Morgan, *Anal. Chem.* **45** (1973) 278A.
- [14] G. Gebel, P. Aldebert and M. Pineri, *Macromolecules* **20** (1987) 1425.
- [15] J. Bett, K. Kinoshita and P. Stonehart, *J. Catal.* **29** (1973) 160.
- [16] E-TEK, Inc., Catalog (1993).
- [17] A. Damjanovic and V. Brusic, *Electrochim. Acta* **12** (1967) 1171.
- [18] A. J. Appleby and B. S. Baker, *J. Electrochem. Soc.* **125** (1978) 404.
- [19] K. Kinoshita, *ibid.* **137** (1990) 845.
- [20] P. Stonehart, 44th ISE Meeting Abstract, Berlin (1993) p. 391.

## Appendix

When the effective electronic conductivity  $\bar{K}_e$  is taken into account, Equation 5 becomes

$$\frac{d\eta}{dx} = \frac{\bar{K} + \bar{K}_e}{\bar{K}\bar{K}_e} j(x) + \frac{i}{\bar{K}_e} \quad (A1)$$

By analogy with Equation 7, the effective electronic conductivity is calculated from its bulk value:

$$\bar{K}_e = \frac{(1 - \theta)}{\tau_e} K_{(\text{bulk})} \quad (A2)$$

where  $\tau_e$  is the tortuosity factor for the electronic conductor phase. The dimensionless differential equation to solve is then

$$\frac{d^2C}{dy^2} = uC \exp \left\{ \frac{v+w}{u} (C-1) + \phi(0) + wIy \right\} \quad (A3)$$

where

$$w = \frac{i_0^* \gamma L \alpha F}{\bar{K}_e RT} \quad (\text{A4})$$

The boundary conditions remain the same (Equations 3(a), 4(a)) and Equation A3 was solved for a fixed value of  $\phi(0) = \phi_s$  by the Runge–Kutta method. In this case computing  $C(0)$ , requires to initially fix arbitrary numerical values to  $C(1)$  and  $I$ , obviously in respect with:  $0 \leq C(1) \leq 1$  and  $0 \leq I \leq \exp(\phi_s)$ . Some iterations allow then determination of the values of  $C(1)$  and  $I$  leading to  $C(0) = 1$ .

When  $\theta \approx 0.5$  (in the active layers used in this work

$\theta = 0.6$ ), the assumption  $\tau \approx \tau_e \approx 1$  is valid. The effective ionic and electronic conductivities are then deduced from equation 7 and (A2):  $\bar{K} \approx 0.6 \times 0.05 = 0.03$  and  $\bar{K}_e \approx (1 - 0.6) \times 20 = 8 \text{ S cm}^{-1}$ . This leads, in Equation A3, to:  $(v + w) \approx v$ .

On the other hand, even for a fast reaction rate (say  $i_0^* = 10^{-3} \text{ A cm}^{-2}$  and  $b = 2.3 RT/\alpha F = 0.03 \text{ V dec}^{-1}$ ), the maximum value of the product ( $w \times I \times y$ ) is  $w \times \exp(\phi_s)$ . At  $\eta_s = 0.1 \text{ V}$ , in an active layer of  $L = 1 \mu\text{m}$  and  $\gamma = 10$ , the calculation provides:  $w \times \exp(\phi_s) \approx 0.02$ , a value much lower than  $\phi_s \approx 7.7$ . If the active layer is finally made of Pt/C and recast Nafion<sup>®</sup> with  $\theta \approx 0.5$ , Equation A3 is reducible to Equation 8.